

Geophysical Research Letters®

RESEARCH LETTER

10.1029/2024GL112409

Key Points:

- Under increasing CO₂, models project extratropical stratospheric ozone to increase except around 10 km (lower dip) and 17 km (upper dip)
- The lower dip is due to expansion of the extratropical troposphere, whereas the upper dip is due to expansion of the tropical troposphere
- Seasonality of the stratospheric overturning circulation helps explain why the lower dip peaks in winter and the upper dip peaks in summer

Supporting Information:

Supporting Information may be found in the online version of this article.

Correspondence to:

A. Match,
aaron.match@cornell.edu

Citation:

Match, A., & Gerber, E. P. (2025). The double dip: How tropospheric expansion counteracts increases in extratropical stratospheric ozone under global warming. *Geophysical Research Letters*, 52, e2024GL112409. <https://doi.org/10.1029/2024GL112409>

Received 5 SEP 2024
Accepted 17 APR 2025

Author Contributions:

Conceptualization: Aaron Match, Edwin P. Gerber

Formal analysis: Aaron Match, Edwin P. Gerber

Funding acquisition: Aaron Match, Edwin P. Gerber

Investigation: Aaron Match, Edwin P. Gerber

Methodology: Aaron Match, Edwin P. Gerber

Project administration: Aaron Match, Edwin P. Gerber

Resources: Aaron Match, Edwin P. Gerber

Software: Aaron Match


Supervision: Edwin P. Gerber

Validation: Aaron Match

© 2025. The Author(s).

This is an open access article under the terms of the [Creative Commons Attribution License](#), which permits use, distribution and reproduction in any medium, provided the original work is properly cited.

The Double Dip: How Tropospheric Expansion Counteracts Increases in Extratropical Stratospheric Ozone Under Global Warming

Aaron Match¹  and Edwin P. Gerber²

¹Department of Earth and Atmospheric Sciences, Cornell University, Ithaca, NY, USA, ²Center for Atmosphere Ocean Science, Courant Institute of Mathematical Sciences, New York University, NY, NY, USA

Abstract In response to rising CO₂, chemistry-climate models (CCMs) project that extratropical stratospheric ozone will increase, except around 10 and 17 km. We call the muted increases or reductions at these altitudes the “double dip.” The double dip results from surface warming (not stratospheric cooling). Using an idealized photochemical-transport model, surface warming is found to produce the double dip via tropospheric expansion, which converts ozone-rich stratospheric air into ozone-poor tropospheric air. The lower dip results from expansion of the extratropical troposphere, as previously understood. The upper dip results from expansion of the tropical troposphere, low-ozone anomalies from which are then transported into the extratropics. Large seasonality in the double dip in CCMs can be explained, at least in part, by seasonality in the stratospheric overturning circulation. The remote effects of the tropical tropopause on extratropical ozone complicate the use of (local) tropopause-following coordinates to remove the effects of global warming.

Plain Language Summary In response to rising atmospheric CO₂ primarily from the burning of fossil fuels, stratospheric ozone in the extratropics tends to increase. These increases result because CO₂ warms the surface, which changes the stratospheric winds, and CO₂ directly cools the stratosphere, which changes chemical reaction rates. However, there are two altitudes where ozone does not increase as much—10 and 17 km—which we term the “double dip.” We find that the double dip exists because the warming of the troposphere allows the tops of rainstorms to reach higher altitudes, reducing stratospheric ozone by injecting ozone-poor tropospheric air. The lower dip results from the deepening of the local, extratropical troposphere. Counterintuitively, the upper dip results from deepening of the faraway tropical troposphere, whose remote reductions in tropical ozone are then transported laterally by the winds into the extratropics. The fact that the double dip depends on both the local and remote deepening of the troposphere complicates a growing practice in ozone trend analysis that only considers the local troposphere.

1. Introduction

The largest anthropogenic effects on the ozone layer have resulted from chemical perturbations due to ozone-depleting substances, but the ozone layer is also being perturbed thermodynamically and dynamically due to rising CO₂. Rising CO₂ leads to both increases and decreases in ozone at different locations, and chemistry-climate models (CCMs) broadly agree on the spatial pattern of this response (e.g., Chiodo et al., 2018; Haigh & Pyle, 1982; Match & Gerber, 2022; Shepherd, 2008). Examples of this robust response are shown from three CCMs in Figure 1. Ozone is simulated to increase in the mid-to upper-stratosphere (i.e., above the ozone maximum), because stratospheric cooling speeds up the three-body reaction that forms O₃ and slows down certain collisional loss reactions (Haigh & Pyle, 1982; Jonsson et al., 2004). Ozone is simulated to decrease in the tropical lower stratosphere for two main reasons: (a) a strengthening of the stratospheric overturning circulation, which upwells ozone-poor air from below (e.g., Li et al., 2009; Shepherd, 2008), and (b) tropospheric expansion, which erodes the ozone layer from below to lead to reductions of ozone that are then upwelled by the climatological overturning (Match & Gerber, 2022).

The ozone response in the extratropical lower stratosphere is less straightforward, as it is not uniform in sign, and, unlike the changes elsewhere, exhibits some sign asymmetries between hemispheres and sign disagreements between models (Figure 1). Nonetheless, a robust vertical structure of the response is evident: although ozone generally increases in the extratropical lower stratosphere under global warming, these increases are punctuated by two “dips” (i.e., reductions in the magnitude of the increase possibly rising to the level of an absolute

Visualization: Aaron Match
Writing – original draft: Aaron Match
Writing – review & editing:
Aaron Match, Edwin P. Gerber

decrease): A lower dip around 10 km and an upper dip around 17 km. We call this response the “double dip.” The double dip exists when averaging either poleward of 30°, where the upper dip might be contaminated by a direct contribution from ozone reductions in the tropical upwelling regime, or when averaging poleward of 60°, far from any tropical contamination (Figure 1, bottom row, solid vs. dashed curves).

The lower dip has been previously described and attributed to tropospheric expansion, which erodes the ozone layer from below by replacing ozone-rich stratospheric air with ozone-poor tropospheric air (Dietmüller et al., 2014; Plummer et al., 2010). The upper dip, on the other hand, has not been the focus of prior work and has not been explicitly discussed despite appearing (sometimes subtly) in figures from numerous previous studies, including Fomichev et al. (2007, their Fig. 12), Shepherd (2008, their Fig. 11), Plummer et al. (2010, their Fig. 2), Dietmüller et al. (2014, their Fig. 1a), Banerjee et al. (2016, their Fig. 1), Chiodo et al. (2018, their Fig. 2), and Keeble et al. (2021, their Fig. 10). Our goals are to explain the mechanisms that lead to the double dip and frame their implications for interpreting ozone trends in the extratropical lower stratosphere.

We begin by analyzing pairs of CMIP6 experiments that isolate the two pathways by which rising CO₂ affects ozone: stratospheric cooling and surface warming. The double dip will be found to result from surface warming (Section 2). Surface warming is proposed to affect stratospheric ozone through tropospheric expansion and by strengthening stratospheric overturning (the latter arguably connected to the former, e.g., as in Oberländer-Hayn et al. (2016), although our analysis treats their effects separately). To disentangle the effects of tropospheric expansion and the strengthening overturning, we analyze a simple photochemical-transport model within which the tropopause height and overturning strength can be independently varied, an extension of models from Match and Gerber (2022) and Match et al. (2024a, 2024b) (Section 3). Our results support previous arguments that the lower dip arises from expansion of the extratropical troposphere (Dietmüller et al., 2014; Plummer et al., 2010) (Section 4). The upper dip also arises from tropospheric expansion, but not of the (local) extratropical troposphere but rather of the (remote) tropical troposphere, reductions in ozone from which are then laterally transported into the extratropics at the altitude of the tropical tropopause around 17 km. We show that the double dip has a strong seasonal cycle in CCMs, which can be reproduced in our simple model as a consequence of seasonality in the overturning, although we do not rule out possible contributions from other seasonal factors (Section 5). We then discuss broad implications of these results for the interpretation of extratropical ozone trends in tropopause-following coordinates (Section 6).

2. The Double Dip: Surface Warming, Not Stratospheric Cooling

The extratropical ozone response to a quadrupling of CO₂ in a pre-industrial atmosphere is shown in Figure 1, and for a quantitative comparison among CCMs in Figure 2a. The increase of CO₂ is thought to affect the ozone layer by perturbing the thermodynamical and dynamical conditions that determine ozone reaction rates and transport. These effects can be distinguished by considering the separate effects of stratospheric cooling and surface warming, whose contributions to the double dip can be assessed by comparing pairs of CCM experiments that isolate each in turn (similar decompositions appear in, e.g., Fomichev et al., 2007; Match & Gerber, 2022). Our pairs of experiments are drawn by opportunity from the CMIP6 archive, a caveat of which is that they have different background states: stratospheric cooling is isolated with respect to a pre-industrial atmosphere, whereas surface warming is isolated with respect to a historical atmosphere (notably including anthropogenic ozone-depleting substances).

Surface warming is isolated by comparing an experiment with sea surface temperatures (SSTs) prescribed according to their historical evolution (amip) versus one in which those historical SSTs are uniformly warmed by 4 K (amip-p4K). Warming the SSTs expands the troposphere and strengthens the overturning but does not directly cool the stratosphere, which occurs under rising CO₂ due to the direct radiative effects of the enhanced CO₂ in the stratosphere (e.g., Manabe & Wetherald, 1967). Figure 2b shows the extratropical ozone response to surface warming in three CCMs. The ozone response to surface warming includes a pronounced double dip, with localized reductions around 10 and 17 km.

To determine whether stratospheric cooling also contributes to the double dip, we isolate its effects by comparing a pre-industrial control (piControl) to a pre-industrial climate with quadrupled CO₂ at fixed SSTs (piClim-4xCO₂). The quadrupled CO₂ cools the stratosphere, but does not warm the troposphere due to the fixed SSTs. Figure 2c shows that stratospheric cooling leads to an increase in extratropical ozone above about 17 km, primarily by perturbing the photochemical reaction rates that produce and destroy ozone. The ozone response in the

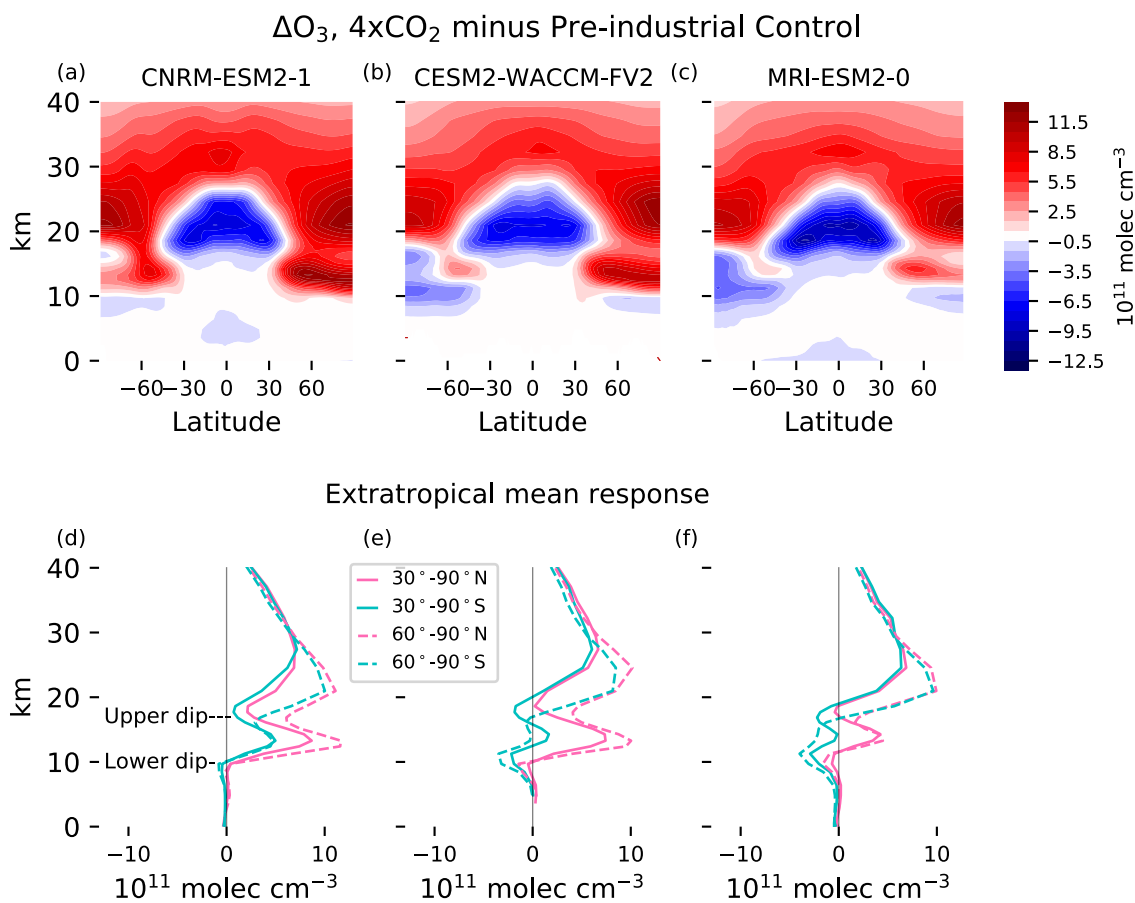


Figure 1. The double dip is evident in the response of extratropical O₃ to a quadrupling of CO₂ in three CMIP6 models with interactive chemistry. Top row: Change in [O₃] in abrupt-4xCO₂ (years 50–150) minus piControl. Bottom row: Extratropical mean changes in [O₃] in the Northern Hemisphere (pink) and Southern Hemisphere (cyan) when averaged poleward of 30° (solid) or 60° (dashed). The lower dip occurs around 10 km, and the upper dip occurs around 17 km.

extratropical lower stratosphere is small and does not project strongly onto either the upper or lower dip. Therefore, we conclude that the double dip results primarily from surface warming.

3. Methods: A Simple Model to Disentangle Contributions From Strengthened Stratospheric Overturning Versus Tropospheric Expansion

Surface warming is hypothesized to lead to the double dip through perturbations in transport. The only mechanism other than transport that has been previously hypothesized to contribute to aspects of the double dip is catalytic chemistry involving anthropogenic ozone-depleting substances. Li and Newman (2023) showed that, in a historical atmosphere in Southern Hemisphere spring, stratospheric cooling from CO₂ could promote the formation of polar stratospheric clouds that exacerbated the upper dip. Although this mechanism seemed important in their simulations, we argue that it is not necessary to explain the upper dip, given that an upper dip is simulated in a pre-industrial background state (Figure 1), it occurs in both hemispheres (not just the Southern Hemisphere, Figure 1), it will be shown to be strongest in summer (not spring) (Section 5), and it will be reproduced in a simple photochemical-transport model driven by transport perturbations alone. Thus, without ruling out possible effects of catalytic chemistry on the double dip in certain contexts, this paper focuses on transport in order to furnish a minimal sufficient explanation of the double dip.

We decompose the effects of transport on ozone into two primary pathways: tropospheric expansion and strengthening of the overturning circulation. Tropospheric expansion results as a direct thermodynamic consequence of global warming (Singh and O’Gorman, 2012; Vallis et al., 2015). A simple scaling for tropospheric expansion of 6 hPa per Kelvin of surface warming was derived in Match and Fueglistaler (2021) by considering

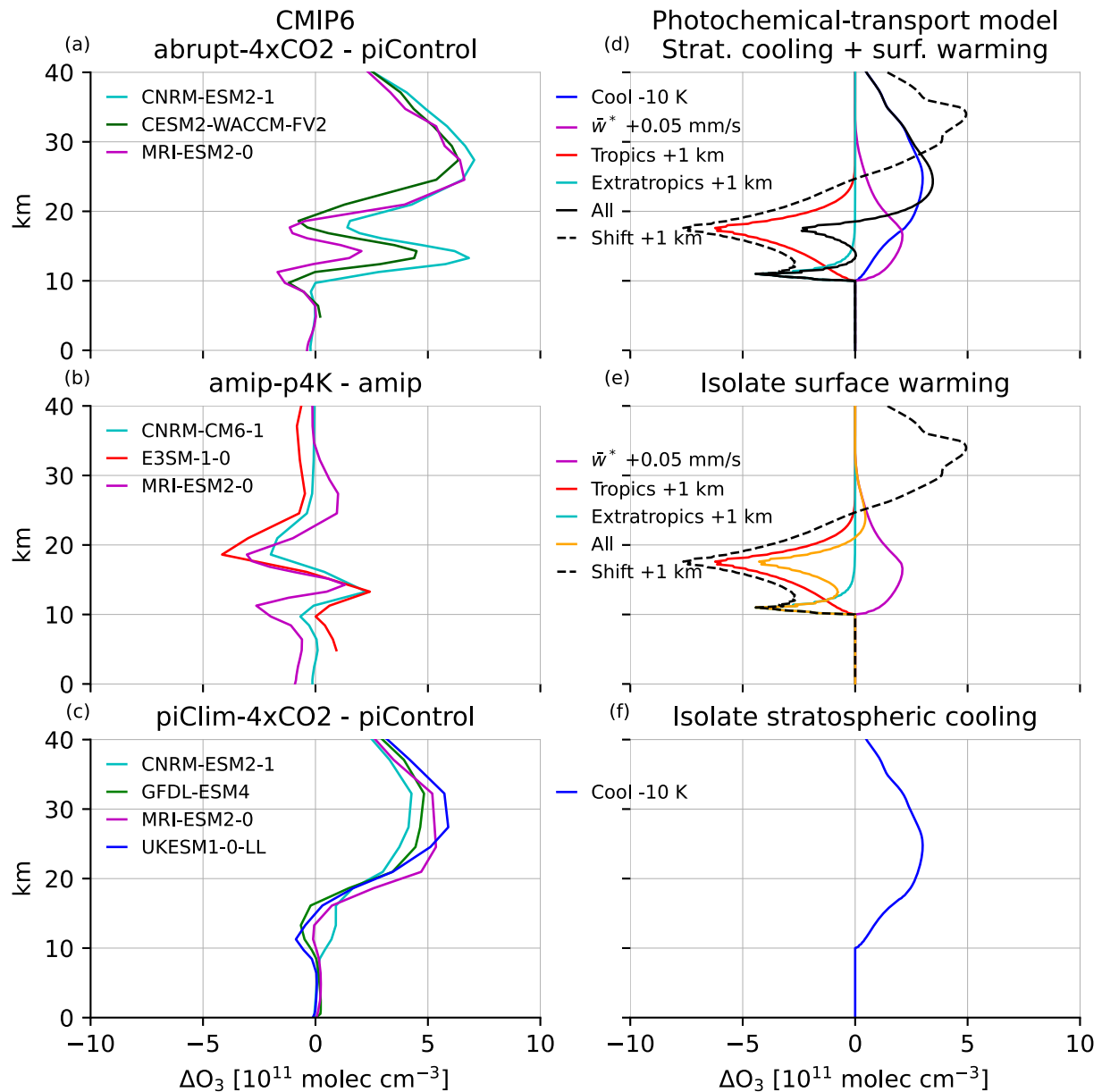


Figure 2. Decomposition of the mechanisms by which increasing CO₂ affects extratropical [O₃] in CMIP6 models (left column) and the simple photochemical-transport model (right column). (a) Response of extratropical [O₃], averaged poleward of 30°, to abrupt-4xCO₂ minus piControl in the three CMIP6 models shown in Figure 1. (b) As above, but isolating surface warming through amip-p4K minus amip. (c) As above, but isolating stratospheric cooling through piClim-4xCO₂ minus piControl. The double dip is due to surface warming and not stratospheric cooling. (Right column) Response of extratropical [O₃] to the key mechanistic drivers: stratospheric cooling of 10 K (blue), strengthening overturning (\bar{w}^*) by 0.05 mm s⁻¹ (magenta), expansion of the tropical troposphere by 1 km (red), expansion of the extratropical troposphere by 1 km (cyan), and all together (black). (Dashed black) Change in [O₃] from a 1 km upward shift of the control ozone profile. The lower dip is due to expansion of the extratropical troposphere, and the upper dip is due to expansion of the tropical troposphere.

that convection must deepen in order for a moist adiabatic parcel launched at the surface to reach an approximately fixed tropopause temperature (Hartmann & Larson, 2002; Jeevanjee & Fueglistaler, 2020; McKim et al., 2024; Seeley et al., 2019). Strengthening of the overturning circulation also roughly scales with surface warming (e.g., Abalos et al., 2021), which Oberländer-Hayn et al. (2016) ascribed to an upward shift of the stratospheric circulation along with the expanding troposphere, although we can assess the effects of strengthening overturning and tropospheric expansion separately. To do so, we formulate a simple photochemical-transport model that distills the processes that control extratropical stratospheric ozone, within which we can separately vary the prescribed tropopause height and overturning strength.

The model is a simple Chapman+2 photochemical-transport model that draws together components of previously-analyzed simple models. Our spectrally-resolved UV photochemistry is based on the Chapman+2 photochemical reactions, which begin with the classical Chapman cycle of ozone photochemistry (Chapman, 1930), but then augment them with generalized sinks of O and O₃ representing catalytic chemistry (as analyzed in Match et al., 2024a, 2024b). The chemical reaction rates are determined by the climatological distribution of catalysts, drawn from a CCM as tabulated in Brasseur and Solomon (2005), and by temperatures, which are assumed for simplicity to be uniform. The Chapman+2 model has previously been described in a single-column steady-state formulation with transport parameterized as a damping, but here transport is instead represented explicitly via a leaky tropical pipe (Match & Gerber, 2022; Neu & Plumb, 1999; Ray et al., 2010; Stolarski et al., 2014). The leaky tropical pipe includes transport by three processes: (a) the overturning (residual mean) circulation, with residual vertical velocity, denoted \bar{w}^* , in each column and meridional velocity between adjacent columns that balances the divergence of the vertical mass flux, (b) lateral two-way mixing between adjacent columns, and (c) vertical diffusion within each column. The lower boundary condition of the model is a prescribed tropopause with zero ozone, as in Match and Gerber (2022). To produce a realistic seasonality of the double dip, our domain has three columns (tropics, Northern Hemisphere extratropics, Southern Hemisphere extratropics), and we impose a seasonal cycle in the strength of the overturning that peaks in the winter in each extratropical hemisphere.

Because our model domain extends down to the extratropical tropopause around 10 km, it must represent transport by the deep branch of the Brewer-Dobson circulation, the shallow branch of the Brewer-Dobson circulation, and stratosphere-troposphere exchange (STE) in the extratropical lowermost stratosphere (e.g., two way exchange by blocking anticyclones, cutoff cyclones, and tropopause folds) (Appenzeller et al., 1996; Gettelman et al., 2011; Holton et al., 1995; Hoor et al., 2004). The shallow branch and STE across the tropopause break are associated with stronger mixing than observed in the stratosphere above, so we prescribe that the lateral mixing rate jumps (step-wise) by a factor of four below the tropical tropopause. This enhanced mixing damps ozone in the extratropical lower stratosphere, and also makes it so that when surface warming shifts the tropical tropopause upwards, the enhanced mixing rates are shifted upwards along with it.

A schematic showing the basic formulation of our simple photochemical-transport model is shown in Figure S1 in Supporting Information S1. A detailed description of the model and our numerical approach is provided in Texts S1 and S2 in Supporting Information S1. The climatological seasonal cycle of ozone in our model is shown in Figure S2 in Supporting Information S1, indicating a favorable comparison to that from the CCM MRI-ESM2-0.

Perturbations are applied to the simple photochemical-transport model to represent the three key effects of quadrupled CO₂. Stratospheric cooling, represented as a uniform cooling of 10 K, perturbs the temperature-dependent reaction rates. Strengthening of the overturning circulation, represented by a seasonally-averaged amplification of the residual vertical velocities (\bar{w}^*) by 0.05 mm s⁻¹, perturbs the net transport by the leaky tropical pipe. Tropospheric expansion, represented by a 1 km upward shift of the tropopause and lateral mixing rates, takes a bite out of the ozone layer from below that is then transported by advection, vertical diffusion, and two-way mixing. Together, these perturbations will be shown to reproduce the response to a quadrupling of CO₂ (see also Match & Gerber, 2022). Critically for our understanding, they can be imposed separately or in various combinations to emulate experiments from the CMIP6 models, allowing us to assess the linearity of the response, and ultimately disentangle the dynamics of the double dip.

For parsimony, our model omits numerous processes that could modulate the double dip or its trends, including (a) a winter polar vortex separated by a mixing barrier and any heterogeneous chemical processing of ozone within the vortex, (b) seasonal cycles in temperature, solar zenith angle, or catalysts, and (c) proposed decadal trends in the latitudinal structure of two-way mixing (Ball et al., 2018, 2020; Orbe et al., 2020; Wargan et al., 2018). As a consequence of this parsimonious approach, our results cannot rule out contributions from mechanisms we did not consider. Nonetheless, we are able to quantitatively reproduce the double dip and interpret its dynamics using experiments that would be impossible in a more highly-coupled model (i.e., in a model within which tropopause height and overturning strength could not be independently varied).

4. Results: The Double Dip Is Due To Tropospheric Expansion

The simple photochemical-transport model is validated by emulating the ozone response in CCMs to (a) surface warming and stratospheric cooling, (b) only surface warming, and (c) only stratospheric cooling, shown in each row of Figure 2. In response to surface warming and stratospheric cooling, ozone generally increases except for the double dip (Figure 2a vs. 2d). Surface warming leads to the double dip without increasing ozone above 20 km (Figure 2b vs. 2e). Stratospheric cooling increases ozone above 20 km without driving the double dip (Figure 2c vs. 2f).

The fact that the simple photochemical-transport model can reproduce results from CCMs builds confidence that it can also further decompose the response to surface warming into distinct contributions from the strengthening overturning and tropospheric expansion, a decomposition which is not possible in the CCMs within which tropopause height and stratospheric overturning are dynamically coupled. The results of this decomposition are shown in Figures 2d and 2e. Consistent with prior literature, expansion of the extratropical troposphere alone (cyan curves) leads directly to the lower dip around 10 km (the climatological altitude of the extratropical tropopause) by eroding the ozone layer from below (Dietmüller et al., 2014; Plummer et al., 2010).

The upper dip arises due to net lateral transport of tropical lower stratospheric ozone reductions into the extratropics. These tropical ozone reductions are shown in Figure S3 in Supporting Information S1, and were found in Match and Gerber (2022) to result from both strengthening overturning and tropospheric expansion. However, these two processes do not contribute equally in the extratropics to the upper dip. This disparity results because the strengthened upwelling in the tropics that leads to reductions of tropical lower stratospheric ozone is accompanied (due to mass continuity) by strengthened downwelling in the extratropics. This strengthening of extratropical downwelling increases extratropical ozone by enhancing the advection of ozone-rich air down from aloft (see also Shepherd, 2008), opposing the formation of the upper dip. In total, strengthened overturning increases extratropical ozone (Figures 2d and 2e, magenta curve).

Rather, the upper dip forms uniquely due to tropical tropospheric expansion (Figures 2d and 2e, red and cyan curves). Tropical tropospheric expansion drives the upper dip by eroding the tropical ozone layer from below, low ozone anomalies from which are then transported upwards into the tropical lower stratosphere (Match & Gerber, 2022) and laterally into the extratropical lower stratosphere. A pathway of lateral mixing from the tropical lower stratosphere into the extratropical lower stratosphere has previously been discussed in other contexts, such as when considering transport of short-lived substances (Bönisch et al., 2009; Gettelman et al., 2011; Hoor et al., 2004) and idealized tracers (Abalos et al., 2017). In our model, tropical tropospheric expansion drives the upper dip in two ways: (a) the upward shift of the ozone-poor tropospheric air, and (b) the upward shift of the two-way mixing rates, which are prescribed to be larger below the tropical tropopause than above it. These two effects both contribute at leading order, as seen in the decomposition of Figure S4 in Supporting Information S1, which considers the extratropical $[O_3]$ response to various combinations of tropospheric expansion (through upward shifts in the tropospheric sink and/or lateral mixing rates) and strengthening overturning.

The upper dip occurs around 17 km because this is the climatological altitude of the tropical tropopause. The vertical separation between the two dips reflects the tropopause break at the subtropical jet, over which the tropopause drops by about 7 km between the tropics and the extratropics. In our model and in the CCMs, the upper dip has larger column-integrated reductions of ozone than the lower dip, suggesting that extratropical column ozone is actually more sensitive to expansion of the faraway tropical tropopause than to expansion of the local tropopause below.

5. Results: Seasonality of the Double Dip

Thus far, we have considered the annually-averaged double dip, but the double dip in CCMs has a strong seasonal cycle. Figure 3a (Northern Hemisphere) and S5a (Southern Hemisphere) show that the lower dip is strongest in winter, whereas the upper dip is strongest in summer and vanishes in winter. This seasonal cycle is evident in both hemispheres and in other CCMs (Figure S6 in Supporting Information S1).

Seasonality of the double dip can be thought of as an interaction between global warming and a seasonally-varying process. Many seasonally-varying processes could facilitate such interactions. Photochemically, there are seasonal cycles in solar zenith angle, catalysts, polar stratospheric clouds, and temperature-dependent reaction rates, among others. Dynamically, there are seasonal cycles in tropopause height, the polar vortex mixing barrier,

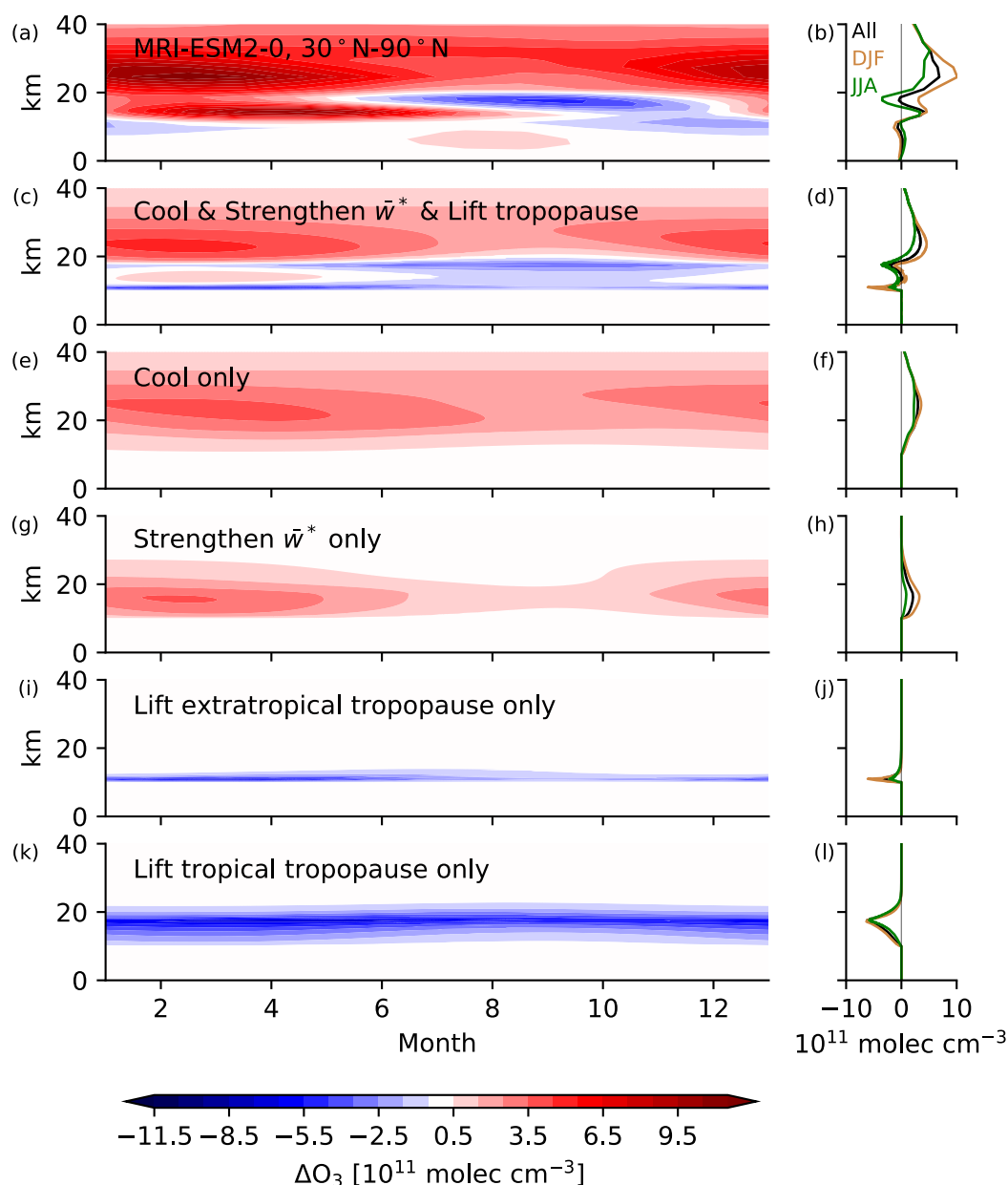


Figure 3. Mechanistic decomposition of the seasonal cycle in the Northern Hemisphere extratropical $[O_3]$ response to global warming. (Left column) (a) MRI-ESM2-0 for abrupt-4xCO₂ minus piControl and (c, e, g, i, k) simple photochemical-transport model mechanism denial experiments, in which all seasonality arises solely from overturning (\bar{w}^*) that peaks in winter. In MRI-ESM2-0, the upper dip around 17 km is strongest in summer whereas the lower dip around 10 km is strongest in winter, with both aspects reproducible from the simple photochemical-transport model whose sole seasonally-varying driver is overturning strength. (Right column) Temporal average of the left column across all months (black), DJF (brown), and JJA (green).

and overturning strength, which is strongest in winter due to the enhanced planetary wave activity propagating up from the troposphere (e.g., Butchart, 2014; Holton et al., 1995). There is also a seasonal cycle in the lateral mixing from the tropical tropopause layer above the subtropical jet into the extratropical lower stratosphere, which maximizes during summer associated with the Asian summer monsoon anticyclone (e.g., Gettelman et al., 2011; Hoor et al., 2004; Stolarski et al., 2014). Yet, we will show that, on its own, a seasonal cycle in overturning is sufficient to reproduce realistic magnitude and phasing of the seasonal cycle in the double dip. Importantly,

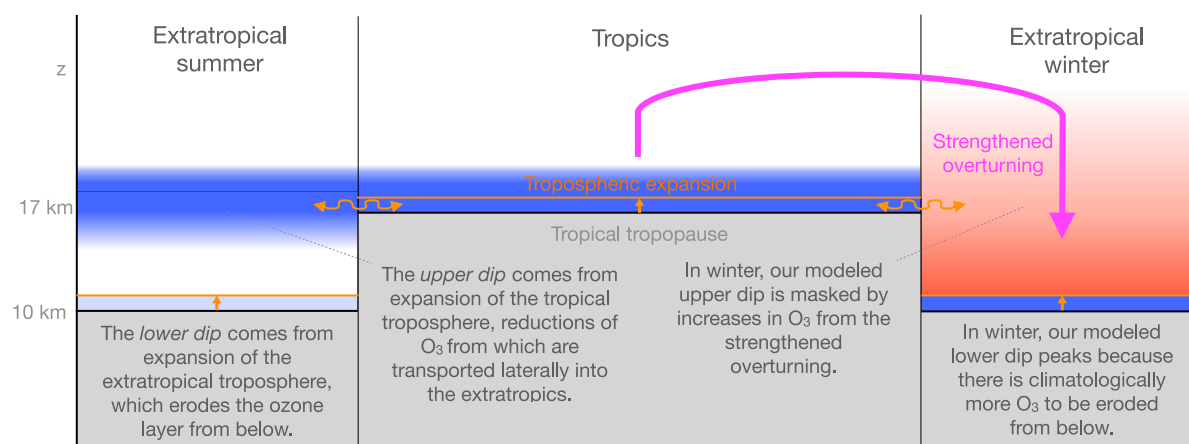


Figure 4. Schematic illustrating how surface warming leads to the double dip and how seasonality in the overturning contributes to seasonality in the double dip in our simple photochemical-transport model. Reductions of ozone are in blue and increases are in red.

though, these results do not rule out possible additional contributions from these other photochemical and dynamical processes.

Figure 3 shows the seasonally-resolved response of NH extratropical ozone to a quadrupling of CO_2 in MRI-ESM2-0. This seasonality has been reproduced in our simple photochemical-transport model, in which the only seasonally-varying boundary condition is the overturning, which varies sinusoidally from zero at the summer solstice to twice the annual mean value at the winter solstice (approximately consistent with reanalyses, e.g., Seviour et al., 2012). In response to this seasonally-varying overturning, the simple photochemical-transport model simulates a lower dip that is stronger in winter and weaker in summer (Figures 3a and 3b), as in the CCMs. The lower dip peaks in winter because that is when lower stratospheric ozone is largest and therefore has the most to lose from extratropical tropospheric expansion. Lower stratospheric ozone is largest during winter due to the strong downwelling, which allows it to accumulate against the primary modeled sink of lateral transport, which represents losses of stratospheric ozone via STE.

The simple photochemical-transport model also has realistic seasonality of the upper dip, which peaks in summer. Interestingly, the modeled seasonality of the upper dip does not come from seasonality in the response to tropical tropospheric expansion, which is actually quite consistent throughout the year (Figures 3k and 3l). Rather, the modeled upper dip peaks in summer because it is seasonally masked by wintertime increases in extratropical ozone due to the wintertime peak in the overturning circulation, which masks the upper dip due to strengthened overturning and stratospheric cooling. Recall that temperature itself is held constant in our model, so the wintertime maximum in response to stratospheric cooling results from advection of the ozone perturbations due to stratospheric cooling by the seasonally-varying (but unperturbed) overturning circulation. A schematic of this mechanistic understanding is shown in Figure 4. We reiterate that, although seasonality of the overturning is sufficient to produce a double dip with realistic amplitude and phase, our analysis has not ruled out possible contributions from other factors, many of which are known to have significant seasonal cycles.

The seasonal cycle of the ozone response to a quadrupling of CO_2 appears to include large cancellation among opposing terms, so it is not surprising that the sign of the ozone response to a quadrupling of CO_2 is not robustly simulated in the lower stratosphere (Figure 1). Although the sign is not robust, this paper demonstrates that key aspects of the pattern of the response, namely the double dip, are robust and can be understood. The sign of the response at each location and throughout the seasonal cycle could be a sensitive indicator for the effects of model disagreements in the response to drivers (e.g., surface warming and stratospheric cooling) and dynamical pathways (e.g., strengthening overturning, tropospheric expansion, two-way mixing).

Rising CO_2 is not the only perturbation that will affect the ozone layer in the coming decades. Ongoing recovery of the ozone hole due to the Montreal Protocol could potentially obscure part of the double dip. Figure S7 in Supporting Information S1 compares ozone in two CCMs (MRI-ESM2-0 and CNRM-ESM2-1) between 2071–2100 and 2015–2044 in the high-development and high-emissions pathway of ssp585. The annually-averaged

change in ozone is plotted as well as the change in only DJF or JJA. Recovery of polar ozone from declining CFCs generally dominates the response, although the upper dip from surface warming is evident in the Northern Hemisphere during JJA for both models.

6. Discussion: Implications for Filtering Global Warming Using Tropopause-Following Coordinates

Filtering out trends in ozone from global warming is of great interest because the residual time series may help reveal the chemical recovery of the ozone layer due to declining ozone-depleting substances (Petropavlovskikh et al., 2019). A growing practice intended to remove the impact of warming is to transform ozone trends into tropopause-following coordinates, based on the understanding that the tropopause rises under global warming (Thompson et al., 2021). The use of tropopause-following coordinates has proceeded with different methods reflecting different assumptions. Some studies assess ozone trends in tropopause-following coordinates through most of the stratosphere (Bognar et al., 2022; Wargan et al., 2018), while others restrict tropopause-following coordinates to an empirically-determined region within roughly 5 km of the tropopause (Hegglin et al., 2008; Millán et al., 2024; Pan et al., 2004). The results in this paper suggest precautions toward each approach.

Using tropopause-following coordinates throughout the stratosphere assumes that ozone is conserved with respect to the local tropopause under dynamical perturbations in tropopause height. Above 25–30 km, however, the ozone layer is typically in photochemical equilibrium (e.g., Brasseur & Solomon, 2005; Match et al., 2024b; Perliski et al., 1989) where it is unaffected by dynamical anomalies in ozone due to local tropopause variability (Match & Gerber, 2022).

Restricting attention to the dynamically-controlled regime below 25–30 km, we have shown that if both the tropical and extratropical tropopauses rise equally, the resulting change in ozone can be approximated by a shift with respect to the local tropopause (Figures 2 and 3, Figure S8 in Supporting Information S1). Yet, this only works for a uniform rise in both tropopauses, which is not necessarily expected in response to warming or in internal variability. Non-uniform tropopause changes introduce problems: if only the tropical tropopause rises, tropopause-following coordinates in the extratropics cannot capture the resulting upper dip (Figure S8b in Supporting Information S1); if only the extratropical tropopause rises, tropopause-following coordinates predict a spurious upper dip (Figure S8c in Supporting Information S1). There does not exist a single tropopause-following coordinate that can filter out arbitrary changes in tropopause structure.

Restricting tropopause-following coordinates to an empirically-determined window near the tropopause can avoid contamination from the photochemically-controlled region, but introduces other challenges. The empirical window is often chosen by using past data of ozone and tropopause heights to identify where tropopause-following coordinates reduce the variance of ozone compared to absolute height coordinates (Hegglin et al., 2008; Millán et al., 2024). This empirical window thus demarcates where the variability in ozone is dominated by variability in extratropical tropopause height, and has generally been found to extend 2–5 km above the extratropical tropopause. Yet, because the empirical window excludes most of the upper dip, a major part of the warming response occurs outside its frame.

7. Conclusions

The extratropical stratospheric ozone response to rising CO₂ has a robust shape: increases in ozone throughout the stratosphere are punctuated by two dips, that is, reductions in the magnitude of increase, potentially large enough to yield absolute reductions. The upper dip is at 17 km and is strongest in summer, and the lower dip is at 10 km and is strongest in winter. With the use of CMIP6 CCM results and a simple photochemical-transport model, the double dip has been explained as follows:

- The lower dip results from expansion of the extratropical troposphere. The lower dip is strongest in winter when extratropical lower stratospheric ozone is largest.
- The upper dip results from expansion of the remote tropical troposphere. The upper dip is strongest in summer, which our simple photochemical-transport model reproduces as a consequence of masking by the strong winter overturning, although other seasonally-varying processes could also be important.

The sensitivity of extratropical lower stratospheric ozone to both local and remote properties of the tropopause complicates the growing practice of using local tropopause-following coordinates to filter out the effects of changes in tropopause height on ozone.

Data Availability Statement

The simple photochemical-transport model, coded in Python, is publicly available at Match (2024), along with the run script used to produce the main experiments analyzed herein. CMIP6 data is freely accessible from <https://esgf-node.llnl.gov/search/cmip6/>.

Acknowledgments

We acknowledge constructive feedback from Peter Hitchcock and two anonymous reviewers. This work was supported by the National Science Foundation under Award No. 2120717 and OAC-2004572, and by Schmidt Sciences, as part of the Virtual Earth System Research Institute (VESRI). For the CMIP6 model output, we acknowledge the World Climate Research Programme, the climate modeling groups, and the Earth System Grid Federation (ESGF), as supported by multiple funding agencies.

References

- Abalos, M., Calvo, N., Benito-Barca, S., Garny, H., Hardiman, S. C., Lin, P., et al. (2021). The Brewer–Dobson circulation in CMIP6. *Atmospheric Chemistry and Physics*, 21(17), 13571–13591. <https://doi.org/10.5194/ACP-21-13571-2021>
- Abalos, M., Randel, W. J., Kinnison, D. E., & Garcia, R. R. (2017). Using the artificial tracer e90 to Examine Present and Future UTLS Tracer Transport in WACCM. *Journal of the Atmospheric Sciences*, 74(10), 3383–3403. <https://doi.org/10.1175/JAS-D-17-0135.1>
- Appenzeller, C., Holton, J. R., & Rosenlof, K. H. (1996). Seasonal variation of mass transport across the tropopause. *Journal of Geophysical Research*, 101(D10), 15071–15078. <https://doi.org/10.1029/96JD00821>
- Ball, W. T., Alsing, J., Mortlock, D. J., Staehelin, J., Haigh, J. D., Peter, T., et al. (2018). Evidence for a continuous decline in lower stratospheric ozone offsetting ozone layer recovery. *Atmospheric Chemistry and Physics*, 18(2), 1379–1394. <https://doi.org/10.5194/acp-18-1379-2018>
- Ball, W. T., Chiodo, G., Abalos, M., Alsing, J., & Stenke, A. (2020). Inconsistencies between chemistry-climate models and observed lower stratospheric ozone trends since 1998. *Atmospheric Chemistry and Physics*, 20(16), 9737–9752. <https://doi.org/10.5194/ACP-20-9737-2020>
- Banerjee, A., Maycock, A. C., Archibald, A. T., Abraham, N. L., Telford, P., Braesicke, P., & Pyle, J. A. (2016). Drivers of changes in stratospheric and tropospheric ozone between year 2000 and 2100. *Atmospheric Chemistry and Physics*, 16(5), 2727–2746. <https://doi.org/10.5194/ACP-16-2727-2016>
- Bognar, K., Tegtmeier, S., Bourassa, A., Roth, C., Warnock, T., Zawada, D., & Degenstein, D. (2022). Stratospheric ozone trends for 1984–2021 in the SAGE II-OSIRIS-SAGE III/ISS composite dataset. *Atmospheric Chemistry and Physics*, 22(14), 9553–9569. <https://doi.org/10.5194/ACP-22-9553-2022>
- Bönisch, H., Engel, A., Curtius, J., Birner, T., & Hoor, P. (2009). Quantifying transport into the lowermost stratosphere using simultaneous in-situ measurements of SF₆ and CO₂. *Atmospheric Chemistry and Physics*, 9(16), 5905–5919. <https://doi.org/10.5194/acp-9-5905-2009>
- Brasseur, G. P., & Solomon, S. (2005). *Aeronomy of the middle atmosphere: Chemistry and Physics of the stratosphere and mesosphere*. Springer.
- Butchart, N. (2014). The Brewer–Dobson circulation. *Reviews of Geophysics*, 52(2), 157–184. <https://doi.org/10.1002/2013RG000448>
- Chapman, S. (1930). A theory of upper atmospheric ozone. *Memoirs of the Royal Meteorological Society*, III(26), 103–125.
- Chiodo, G., Polvani, L. M., Marsh, D. R., Stenke, A., Ball, W., Rozanov, E., et al. (2018). The response of the ozone layer to quadrupled CO₂ concentrations. *Journal of Climate*, 31(10), 3893–3907. <https://doi.org/10.1175/JCLI-D-17-0492.1>
- Dietmüller, S., Ponater, M., & Sausen, R. (2014). Interactive ozone induces a negative feedback in CO₂-driven climate change simulations. *Journal of Geophysical Research: Atmospheres*, 119(4), 1796–1805. <https://doi.org/10.1002/2013JD020575>
- Fomichev, V. I., Jonsson, A. I., de Grandpré, J., Beagley, S. R., McLandress, C., Semeniuk, K., & Shepherd, T. G. (2007). Response of the middle atmosphere to CO₂ doubling: Results from the Canadian middle atmosphere model. *Journal of Climate*, 20(7), 1121–1144. <https://doi.org/10.1175/JCLI4030.1>
- Gettelman, A., Hoor, P., Pan, L. L., Randel, W. J., Hegglin, M. I., & Birner, T. (2011). The extratropical upper troposphere and lower stratosphere. *Reviews of Geophysics*, 49(3). <https://doi.org/10.1029/2011RG000355>
- Haigh, J. D., & Pyle, J. A. (1982). Ozone perturbation experiments in a two-dimensional circulation model. *Quarterly Journal of the Royal Meteorological Society*, 108(457), 551–574. <https://doi.org/10.1002/QJ.49710845705>
- Hartmann, D. L., & Larson, K. (2002). An important constraint on tropical cloud - Climate feedback. *Geophysical Research Letters*, 29(20), 12-1–12-4. <https://doi.org/10.1029/2002gl015835>
- Hegglin, M. I., Boone, C. D., Manney, G. L., Shepherd, T. G., Walker, K. A., Bernath, P. F., et al. (2008). Validation of ACE-FTS satellite data in the upper troposphere/lower stratosphere (UTLS) using non-coincident measurements. *Atmospheric Chemistry and Physics*, 8(6), 1483–1499. <https://doi.org/10.5194/acp-8-1483-2008>
- Holton, J. R., Haynes, P. H., McIntyre, M. E., Douglass, A. R., Rood, R. B., & Pfister, L. (1995). Stratosphere-troposphere exchange. *Reviews of Geophysics*, 33(4), 403. <https://doi.org/10.1029/95RG02097>
- Hoor, P., Gurk, C., Brunner, D., Hegglin, M. I., Wernli, H., & Fischer, H. (2004). Seasonality and extent of extratropical TST derived from in-situ CO measurements during SPURT. *Atmospheric Chemistry and Physics*, 4(5), 1427–1442. <https://doi.org/10.5194/acp-4-1427-2004>
- Jeevanjee, N., & Fueglistaler, S. (2020). Simple spectral models for atmospheric radiative cooling. *Journal of the Atmospheric Sciences*, 77(2), 479–497. <https://doi.org/10.1175/JAS-D-18-0347.1>
- Jonsson, A. I., de Grandpré, J., Fomichev, V. I., McConnell, J. C., & Beagley, S. R. (2004). Doubled CO₂ -induced cooling in the middle atmosphere: Photochemical analysis of the ozone radiative feedback. *Journal of Geophysical Research*, 109(D24), D24103. <https://doi.org/10.1029/2004JD005093>
- Keeble, J., Hassler, B., Banerjee, A., Checa-Garcia, R., Chiodo, G., Davis, S., et al. (2021). Evaluating stratospheric ozone and water vapour changes in CMIP6 models from 1850 to 2100. *Atmospheric Chemistry and Physics*, 21(6), 5015–5061. <https://doi.org/10.5194/ACP-21-5015-2021>
- Li, F., & Newman, P. A. (2023). Prescribing stratospheric chemistry overestimates southern hemisphere climate change during austral spring in response to quadrupled CO₂. *Climate Dynamics*, 61(3), 1105–1122. <https://doi.org/10.1007/s00382-022-06588-4>
- Li, F., Stolarski, R. S., & Newman, P. A. (2009). Stratospheric ozone in the post-CFC era. *Atmospheric Chemistry and Physics*, 9(6), 2207–2213. <https://doi.org/10.5194/ACP-9-2207-2009>
- Manabe, S., & Wetherald, R. T. (1967). Thermal equilibrium of the atmosphere with a given distribution of relative humidity. *Journal of the Atmospheric Sciences*, 24(3), 241–259. [https://doi.org/10.1175/1520-0469\(1967\)024<0241:TEOTAW>2.0](https://doi.org/10.1175/1520-0469(1967)024<0241:TEOTAW>2.0)
- Match, A. (2024). Chapman+2 photochemical-transport model [software]. Zenodo. <https://doi.org/10.5281/zenodo.13412270>

- Match, A., & Fueglistaler, S. (2021). Large internal variability dominates over global warming signal in observed lower stratospheric QBO amplitude. *Journal of Climate*, *34*(24), 9823–9836. <https://doi.org/10.1175/JCLI-D-21-0270.1>
- Match, A., & Gerber, E. P. (2022). Tropospheric expansion under global warming reduces tropical lower stratospheric ozone. *Geophysical Research Letters*, *49*(19), e2022GL099463. <https://doi.org/10.1029/2022GL099463>
- Match, A., Gerber, E. P., & Fueglistaler, S. (2024a). Beyond self-healing: Stabilizing and destabilizing photochemical adjustment of the ozone layer. *Atmospheric Chemistry and Physics*, *24*(18), 10305–10322. <https://doi.org/10.5194/acp-24-10305-2024>
- Match, A., Gerber, E. P., & Fueglistaler, S. (2024b). *Protection without poison: Why tropical ozone maximizes in the interior of the atmosphere* (pp. 1–29). EGU sphere. <https://doi.org/10.5194/egusphere-2024-1552>
- McKim, B. A., Jeevanjee, N., Vallis, G. K., & Lewis, N. T. (2024). Water vapor spectroscopy and thermodynamics constrain Earth's tropopause temperature (Preprint). *Preprints*. <https://doi.org/10.22541/essoar.170904795.55675140/v1>
- Millán, L. F., Hoor, P., Hegglin, M. I., Manney, G. L., Boenisch, H., Jeffery, P., et al. (2024). Exploring ozone variability in the upper troposphere and lower stratosphere using dynamical coordinates. *Atmospheric Chemistry and Physics*, *24*(13), 7927–7959. <https://doi.org/10.5194/acp-24-7927-2024>
- Neu, J. L., & Plumb, R. A. (1999). Age of air in a “leaky pipe” model of stratospheric transport. *Journal of Geophysical Research*, *104*(D16), 19243. <https://doi.org/10.1029/1999JD900251>
- Oberländer-Hayn, S., Gerber, E. P., Abalichin, J., Akiyoshi, H., Kerschbaumer, A., Kubin, A., et al. (2016). Is the Brewer-Dobson circulation increasing, or moving upward? *Geophysical Research Letters*, *1772*–1779. <https://doi.org/10.1002/2015GL067545>
- Orbe, C., Wargan, K., Pawson, S., & Oman, L. D. (2020). Mechanisms linked to recent ozone decreases in the Northern hemisphere lower stratosphere. *Journal of Geophysical Research: Atmospheres*, *125*(9), e2019JD031631. <https://doi.org/10.1029/2019JD031631>
- Pan, L. L., Randel, W. J., Gary, B. L., Mahoney, M. J., & Hints, E. J. (2004). Definitions and sharpness of the extratropical tropopause: A trace gas perspective. *Journal of Geophysical Research*, *109*(D23). <https://doi.org/10.1029/2004JD004982>
- Perliski, L. M., Solomon, S., & London, J. (1989). On the interpretation of seasonal variations of stratospheric ozone. *Planetary and Space Science*, *37*(12), 1527–1538. [https://doi.org/10.1016/0032-0633\(89\)90143-8](https://doi.org/10.1016/0032-0633(89)90143-8)
- Petropavlovskikh, I., Godin-Beekmann, S., Hubert, D., Damadeo, R., Hassler, B., & Sofieva, V. (2019). SPARC/I03C/GAW report on long-term ozone trends and uncertainties in the stratosphere. (*Tech. Rep.*) SPARC/I03C/GAW.
- Plummer, D. A., Scinocca, J. F., Shepherd, T. G., Reader, M. C., & Jonsson, A. I. (2010). Quantifying the contributions to stratospheric ozone changes from ozone depleting substances and greenhouse gases. *Atmospheric Chemistry and Physics*, *10*, 8803–8820. <https://doi.org/10.5194/acp-10-8803-2010>
- Ray, E. A., Moore, F. L., Rosenlof, K. H., Davis, S. M., Boenisch, H., Morgenstern, O., et al. (2010). Evidence for changes in stratospheric transport and mixing over the past three decades based on multiple data sets and tropical leaky pipe analysis. *Journal of Geophysical Research*, *115*(D21). <https://doi.org/10.1029/2010JD014206>
- Seeley, J. T., Jeevanjee, N., & Roms, D. M. (2019). FAT or FiTT: Are anvil clouds or the tropopause temperature invariant? *Geophysical Research Letters*, *46*(3), 1842–1850. <https://doi.org/10.1029/2018GL080096>
- Seviour, W. J. M., Butchart, N., & Hardiman, S. C. (2012). The Brewer-Dobson circulation inferred from ERA-Interim. *Quarterly Journal of the Royal Meteorological Society*, *138*(665), 878–888. <https://doi.org/10.1002/qj.966>
- Shepherd, T. G. (2008). Dynamics, stratospheric ozone, and climate change. *Atmosphere-Ocean*, *46*(1), 117–138. <https://doi.org/10.3137/ao.460106>
- Singh, M. S., & O’Gorman, P. A. (2012). Upward shift of the atmospheric general circulation under global warming: Theory and simulations. *Journal of Climate*, *25*(23), 8259–8276. <https://doi.org/10.1175/JCLI-D-11-00699.1>
- Stolarski, R. S., Waugh, D. W., Wang, L., Oman, L. D., Douglass, A. R., & Newman, P. A. (2014). Seasonal variation of ozone in the tropical lower stratosphere: Southern tropics are different from northern tropics. *Journal of Geophysical Research: Atmospheres*, *119*(10), 6196–6206. <https://doi.org/10.1002/2013JD021294>
- Thompson, A. M., Stauffer, R. M., Wargan, K., Witte, J. C., Kollonige, D. E., & Ziemke, J. R. (2021). Regional and seasonal trends in tropical ozone from SHADOZ profiles: Reference for models and satellite products. *Journal of Geophysical Research: Atmospheres*, *126*(22), e2021JD034691. <https://doi.org/10.1029/2021JD034691>
- Vallis, G. K., Zurita-Gotor, P., Cairns, C., & Kidston, J. (2015). Response of the large-scale structure of the atmosphere to global warming. *Quarterly Journal of the Royal Meteorological Society*, *141*(690), 1479–1501. <https://doi.org/10.1002/qj.2456>
- Wargan, K., Orbe, C., Pawson, S., Ziemke, J. R., Oman, L. D., Olsen, M. A., et al. (2018). Recent decline in extratropical lower stratospheric ozone attributed to circulation changes. *Geophysical Research Letters*, *45*(10), 5166–5176. <https://doi.org/10.1029/2018GL077406>

References From the Supporting Information

- Ackerman, M. (1971). *Ultraviolet solar radiation related to mesospheric processes*. (pp. 149–159). Springer. https://doi.org/10.1007/978-94-010-3114-1_11
- Bates, D. R., & Nicolet, M. (1950). The photochemistry of atmospheric water vapor. *Journal of Geophysical Research*, *55*(3), 301–327. <https://doi.org/10.1029/JZ055i003p00301>
- Coddington, O., Lean, J., Lindholm, D., Pilewskie, P., & Snow, M. (2015). NOAA climate data record (CDR) of solar spectral irradiance (SSI). *NOAA CDR Program*. <https://doi.org/10.7289/V53776SW>
- Crutzen, P. J. (1970). The influence of nitrogen oxides on the atmospheric ozone content. *Quarterly Journal of the Royal Meteorological Society*, *96*(408), 320–325. <https://doi.org/10.1002/qj.49709640815>
- Plumb, R. A. (1996). A “tropical pipe” model of stratospheric transport. *Journal of Geophysical Research*, *101*(D2), 3957. <https://doi.org/10.1029/95JD03002>
- Sander, S. P., Abbatt, J., Barker, J. R., Burkholder, J. B., Friedl, R. R., Golden, D. M., et al. (2010). *Chemical kinetics and photochemical data for use in atmospheric studies, evaluation No. 17 (Tech. Rep. No. 10-6)*. Jet Propulsion Laboratory.